SRI CAT NEWSLETTER

Synchrotron Radiation Instrumentation Collaborative Access Team Newsletter
Vol. 1, No. 2 **October 1994**

From the desk of the Executive Director:

Well, anyone who has been in the halls of building 362 knows the pace of activities in the SRI CAT, and in all of XFD for that matter, has markedly increased over the last several months. One recent accomplishment has been the completion of our responses to all the actions items brought up by the committee reviewing our Preliminary Design Report (PDR). We have already begun work on the Final Design Report (FDR) and are planning a submission date in the near future. During the next several months, we will move from the era of writing procurement packages and developing design reports to installing actual hardware on the Experiment Hall floor, a much more gratifying task for experimentalists. We are pushing very hard to be in a position to accept radiation into the 1-BM first optics enclosure very soon after commissioning of the storage ring has started. This will depend on the delivery of several key items, and we are already pushing the vendors to deliver on an accelerated schedule.

After an enormous amount of planning and preparation, the first piece of SRI CAT hardware has been installed on the Experiment Hall floor - a monochromatic beam experimental station for the 1-ID line. We plan to fully outfit this station with utilities, racks, Personnel Safety System (PSS), etc., so that it might serve as an example for installation of future hutches.

Things are moving along not just for the SRI CAT but for many of the other APS CATs as well. Members of the SRI CAT feel this gearing up indirectly as pressure to serve on committees to help set experimental policies and procedures, and to get out reports and technical bulletins stating those policies in a timely fashion. I know these activities take away from your primary responsibilities, but they are important for the entire user community, and I would like to thank you for giving your valuable time to these efforts.

We had planned to have a CAT-wide meeting here at ANL on November 4, 1994 to discuss the planned installation and commissioning schedule of the SRI CAT beamlines and begin planning of the initial experiments. However, the nuclear resonant scattering group recently received beamtime in Japan during this time, and we are now planning to postpone the SRI CAT meeting until Monday, November 21, 1994. We are sending out, under separate cover, a letter noting the change of date and tentative agenda (perhaps you have already received it).

Oh, by the way, I would like to thank all the people who spent their valuable time and effort in designing an SRI CAT logo. We will decide on a winner and let you know the outcome in the next edition of the Newsletter. *D.M. Mills* ❖

The first station in the Experiment Hall begins to take shape. Assembly of this monochromatic station located on the 1ID line should be complete by the end of October. It represents a major milestone in our SRI CAT construction process since it is the first piece of hardware for the SRI CAT beamline to be installed on the Experiment Hall floor at the APS.

X-ray Physics Group Activities

Although the scientific interests of the SRI CAT members based at ANL are probably well known by now, that same statement may not hold true for non-APS members of *(continued on page 2)*

Contents

From the Desk	1
X-ray Physics Group Activities	1
First Undulator	3
Calendar	5
Vacuum Protection of Beamline Front Ends	6
New People	8
Publications	8

SRI CAT, in particular those interests of the X-ray Physics Group (XRPG). To update everyone, several members of the XRPG have listed their current research interests and activities, and have agreed to provide descriptions of their latest research interests and activities, to be divulged in the SRI CAT Newsletter.

R. COLELLA is interested in quasicrystals. One issue under investigation is whether or not quasicrystals possess a center of inversion. Three-beam diffraction experiments can provide the phases of Bragg reflections, which are not in general consistent with centrosymmetry. Good data have been obtained on icosahedral Al-Pd-Mn, and more recently on Al-Cu-Co, a decagonal quasicrystal. On the other hand, standard two-beam diffraction results are in support of centrosymmetry; so, there is a problem there to be solved.

Another aspect of Colella's research concerning quasicrystals has to do with dynamical diffraction in Al-Pd-Mn crystalline specimens, which can be obtained in large dimensions, with virtually zero mosaic spread. Structure factors are being measured on an absolute basis for comparison with theory, and anomalous transmission will be investigated in detail, following up on the work by Kycia et al. (Phys. Rev. B 48, 3544 (1993)).

In a different context, a collaborative effort is being initiated with some other members of the SRI CAT (E. Alp and others) on resonant nuclear scattering. A graduate student from Purdue will be working at the APS, starting in January 1995, and will perform his Ph.D. thesis work *"in absentia"* under Colella and Alp's joint supervision.

Q. SHUN's interests are divided between: (1) diffusion and strain effect in periodic nano-structures on singly-crystal semiconductor surfaces, and (2) magnetic ordering in crystalline materials, such as MBE-grown zinc-blend Mn chalcogenides (*e.g.*, $Zn_{1-x}Mn_xTe$), using polarization-sensitive x-ray scattering and spectroscopy.

(1) Periodic arrays of nano-structures of sizes 1 to 100 nm on semiconductor surfaces have attracted great interest because of their unusual quantum-confined electron properties and their potential applications in electronic and optoelectronic devices. These nano-structure arrays also serve to model rough surfaces with a predominant spatial frequency for studying atomic kinetics involving mass transport, surface diffusion and step arrangements. In collaboration with J.M. Blakely's group in the MS&E Department at Cornell, Shen has developed an x-ray surface-scattering program, and one of his current interests is to study the structure of the surface nano-arrays and their evolution under high temperature annealing and oxidization using x-ray diffraction.

(2) With the advent of intense synchrotron sources, it has become evident that x-ray scattering and spectroscopy play an important role in the study of magnetic structures. Special polarization dependence, element-specific resonant enhancement, high resolution in momentum transfer, and surface sensitivity make x-ray techniques complementary to traditional neutron scattering probes. Shen's recent research activities in polarization-related x-ray science, such as phase plates, Stokes polarimetry, multibeam diffraction, and resonant scattering, reflect his interests in this area. In particular, he would like to utilize x-ray scattering to obtain new information that is not readily available with neutrons. For example, elastic neutron scattering on MBE grown $Zn_{1-x}Mn_xTe$ showed a long-range antiferromagnetic order below 60 K. It could not be determined, however, whether the spins were lined up collinearly or rotated by 90°. This ambiguity can be resolved with x-ray magnetic scattering because the scattering cross-section depends on both the spin and the polarization directions, which affect the strengths of magnetic reflections differently compared to neutrons. By tuning the x-ray energy to the Zn and Mn K-edges, it may be possible to determine separate contributions to the magnetism from each element.

STEVE DURBIN: Recent efforts include developing the original Darwin theory of diffraction into a useful form for many modern dynamical diffraction geometries. This is a numerical technique that does not rely on any underlying periodicity in the "crystal", which makes it well-suited for modeling, for example, the reflectivity of surface monolayers on bulk substrates supporting arbitrary heterostructures grown by MBE techniques, and crystals with lattice parameter variations caused by bending. We are currently applying it to the reflectivity of low-temperature GaAs, a remarkable material that diffracts like a perfect crystal despite extremely high interstitial arsenic concentrations. We are also investigating the dynamical diffracting properties of quasicrystals and have calculated for the first time the exact Darwin reflectivity curve for a quasicrystal, which has all of the characteristic features seen with perfect periodic crystals. ❖

SRI CAT

Synchrotron Radiation Instrumentation
Collaborative Access Team
Argonne National Laboratory
9700 South Cass Avenue
Argonne Il 60439

Executive Director
Dennis M. Mills
Program Directors
Efim Gluskin
Roberto Colella
Associate Directors
Richard Hewitt
Deming Shu
SRI CAT Secretary
Cheryl Zidel
Phone: 708-252-7366
Fax: 708-252-3222
e-mail:
Zidel@anlaps.aps.anl.gov
Newsletter Coeditors
Albert T. Macrander
Ian McNulty

Address additions, changes and deletions are welcome. Forward them to the SRI CAT Secretary.

Next Issue - January 1995

The First Undulator A Has Arrived!!

The first Undulator A, manufactured by STI Optronics of Bellevue, Washington, arrived at the APS on August 9, 1994. By the end of the day, it had been uncrated and installed in the magnetic measurement room. Figure 1 is a photograph of the installed undulator.

A long list of acceptance tests was subsequently run on the undulator, including physical measurements of the device, testing the various motions, and extensive measurements of the magnetic field. The undulator was found to be satisfactory and was formally accepted on August 31.

Some of the first tests came during the mounting of the new insertion device undulator in the magnetic measurement room. The undulator was installed in the room in the same way that it will be installed in the storage-ring tunnel. A base to support it had already been prealigned and bolted to the floor. After the undulator was removed from its shipping crate, two riggers (a third helped steer) rolled it on its wheels into the measurement room. It was rolled into place over the base, then the wheels were raised and the undulator was lowered into its position on the base. Fine position adjustment is built into the undulator support; that adjustment was found to be very smooth and convenient to operate. With a little experience, which will be gained both by installing a few undulators in the measurement room for acceptance measurements and by an early test installation in the storage ring, the installation of the undulators in the storage ring is expected to proceed smoothly and rapidly.

The most important of the acceptance tests, however, were those to characterize the magnetic field. STI had measured the magnetic field of the undulator very thoroughly before shipping it. Measurements were also made at the APS after the undulator's arrival. There was reasonable agreement between these sets of measurements, so we were confident that no damage occurred during shipping. Measurements were made of both the vertical and horizontal components of the field along the center of the undulator, as well as along lines offset horizontally from the center line. Measuring devices included a scanning Hall probe, a scanning coil that was about half as long as the 3.3-cm period of the undulator, and a long rotating coil that stretched the entire length of the undulator, with enough extra included at the ends to include the end fields in the measurements. These measurements were used to determine:

- The peak and effective fields at minimum gap. The effective field determines the energies of the harmonics in the emitted x-ray spectrum. The peak field is used for calculations of the power in the photon beam.
- The first integral of the field through the undulator. A nonzero first integral causes a positron that has passed through the undulator to be traveling in a direction different from its initial direction. This change in direction can affect the position and/or direction of the trajectory of that positron elsewhere in the ring and on future circuits of the ring. The overall result is a distortion in the closed orbit of the positron beam as a whole, with the distortions not necessarily being limited to the immediate vicinity of the undulator. The need to keep the positron beam in the storage ring stable therefore imposes maximum allowed values on both the vertical and horizontal components.
- The second integral of the field through the undulator. A nonzero second integral causes a positron that has passed through the undulator to have a trajectory that is offset from its incident trajectory. Again, this will cause a distortion in the closed orbit of the positron beam; therefore, storage-ring beam stability requirements impose maximum allowed values on both the vertical and horizontal components.
- The normal and skew integrated quadrupole, sextupole, and octupole components of the field. These describe how the integral of the magnetic field through the undulator varies as the line of integration is moved vertically or laterally. They affect the differences in what happens to individual positrons that are still within the positron beam but that have slightly different incident positions, angles, and/or energies. To be more specific, the quadrupole integral will affect the tune of the storage ring — the number of oscillations that an individual positron makes about its equilibrium trajectory as it goes around the storage ring. A skew quadrupole integral results in coupling between the vertical and horizontal beam motions, which for the APS means an increase in the vertical beam size. The sextupole and octupole integrals affect the dynamic aperture. Positrons that stray outside

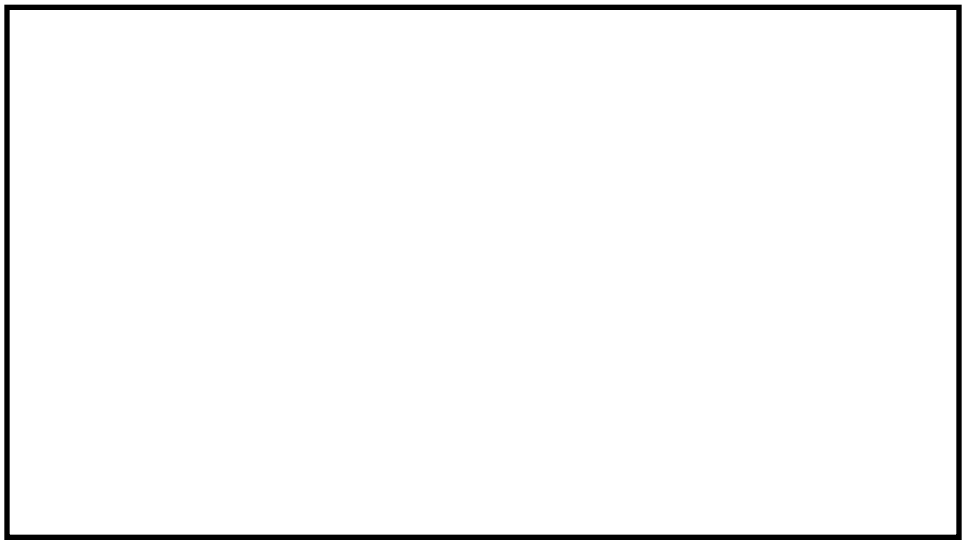

Fig. 1. Jenny O'Brien with the first Undulator A. The undulator is installed in the magnetic measurement room and ready for characterization. The granite magnet measurement bench is in the foreground. The scanning platform that carries the Hall probe or short coil is immediately in front of Jenny.

the dynamic aperture are lost from the beam. Both skew and normal sextupole and octupole integrals that are too big will reduce the dynamic aperture and cause a decrease in beam lifetime. Storage-ring considerations set maximum allowable values on these quantities.

- Transverse roll-off. If the field strength falls off too rapidly in a lateral direction from the center line through the undulator, then the x-ray spectrum will vary if the positron trajectory through the undulator differs laterally.
- Phase error. The trajectory of a positron through the undulator is approximately sinusoidal. The x-radiation emitted by the positron consists of pulses emitted when the acceleration of the positron is greatest or at the peaks in the sine wave. It is the interference between these pulses that produces the sharply peaked undulator spectrum. If an error in the magnetic field results in a variation in the time the positron takes between successive emitted x-ray pulses, it will degrade the peak brilliance. The decrease in brilliance is more pronounced at higher harmonics. The trajectory of a positron is calculated by integrating the magnetic field along the undulator axis, then multiplying by a factor to take beam rigidity into account; the calculated trajectory for this undulator at a gap of 11.5 mm is shown in Fig. 2.
- Peak field variation. A variation in the strength of the peaks of the magnetic field will contribute to the phase error.
- Trajectory straightness and angle. A variation in angle of the trajectory means that the direction of emission of the most intense "on-axis" radiation will vary for different parts of the undulator. This would affect the brilliance and might broaden the undulator spectrum peaks.

While all of these magnetic field requirements are important, the aspects of the field quality that are of particular relevance to users are: the field strength and therefore the range of available photon energies, how good the emitted x-ray spectrum will be, and whether the effect of the undulator on the stored beam will be sufficiently independent of gap to allow users the freedom to change the gap freely. The stringent specifications for the undulators were set to ensure that these aspects of the field quality would be acceptable. The specifications were quite demanding given the current state of the art. The first Undulator A now exceeds these requirements. The predictions for the first Undulator A will be discussed below, based on the magnetic field measurements.

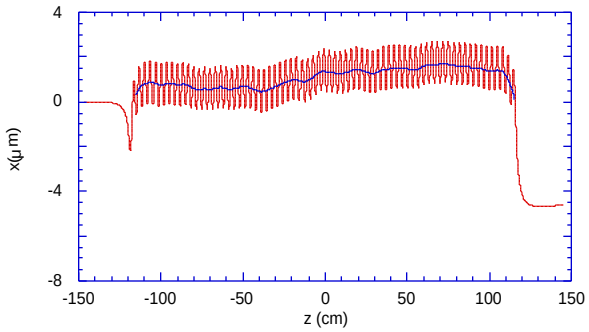

Fig. 2. Horizontal trajectory of a positron through the undulator, calculated using the measured magnetic field. The trajectory after averaging over a period length to remove the periodic wiggles is also shown. The field measurements were made at a gap of 11.5 mm, where the first harmonic energy is 3.4 keV.

Measurements of the magnetic field as a function of position along the axis of the undulator are used to determine the effective field. These measurements were made at a number of different gaps; results of a set of such measurements are shown in Fig. 3, with a curve that approximates the effective field for an undulator that merely met the minimum specified field requirement. As can be seen, the undulator produces a larger field than the minimum. This means that smaller first-harmonic photon energies will be attainable; instead of the promised 3.3-keV minimum first harmonic energy, 2.9 keV will be possible.

A nearly ideal emitted spectrum can best be guaranteed by requiring that the phase error be small. The Undulator A specification required a maximum of 8 degrees of rms phase error. STI did a lot of tuning of the magnetic field of the undulator in order to achieve a small phase error. They more than met the requirement: the phase error achieved was less than 5 degrees.

Calculations of the x-ray spectrum made from the measured magnetic field predict a very high quality spectrum. The specifications for the undulator were written to ensure that the brilliance of the third harmonic would be at least 70% of the brilliance of an ideal undulator. The results for the first Undulator A are

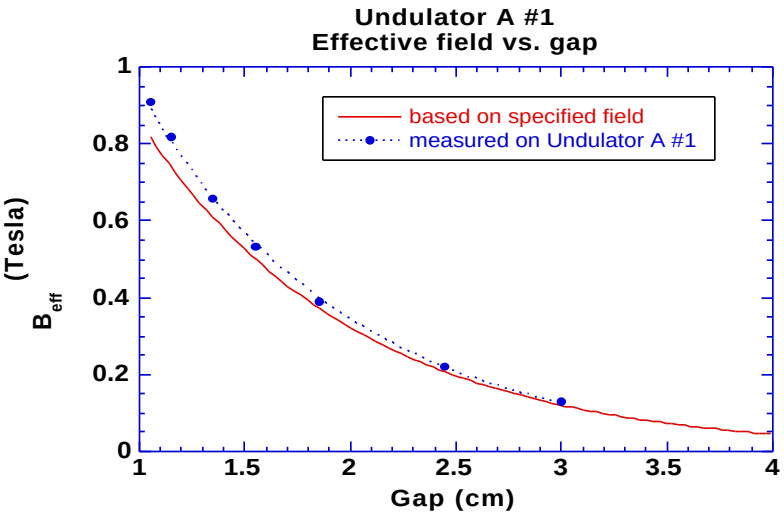

Fig. 3. Effective field of the undulator as a function of gap. The actual field exceeds the specified field so that the first harmonic peak will be able to be tuned to as low as 2.9 keV instead of the expected 3.3 keV. The dotted line is an exponential fit to the measured data.

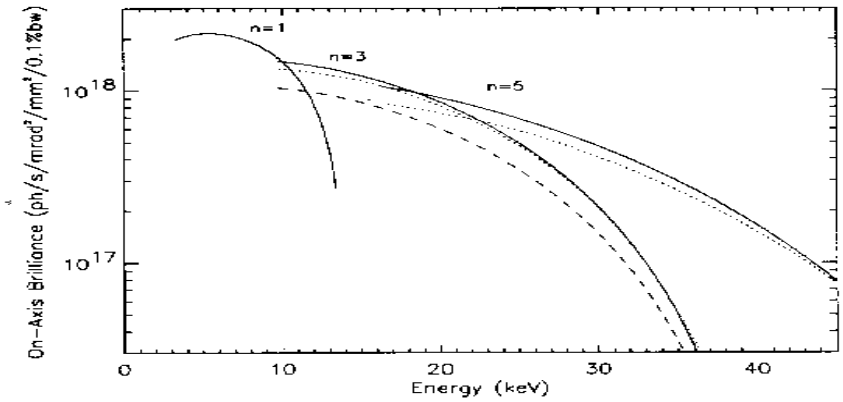

Fig. 4. On-axis brilliance expected from the undulator as a function of energy. The dotted lines show the brilliance curve for the undulator, calculated from measurements of the field both as a function of position along the undulator and as a function of gap, taking into account the emittance of the positron beam. The solid lines show tuning curves for an ideal device; the dashed line shows a tuning curve for an undulator that only just meets the original technical specification. Curves are included for first, third, and fifth harmonics for the ideal and real undulators. (The first harmonic curves for the real and ideal devices are indistinguishable on this scale.)

far better. When the emittance of the storage ring is taken into account, the brilliance of the third harmonic is 93% of that for an ideal undulator, and the fifth harmonic is 80% of ideal. Therefore, the fifth harmonic radiation will be usable, not just the first and third as originally intended. The comparison with the ideal case is even better if the total flux through an aperture that is 2.5 mm horizontally by 1 mm vertically at a distance of 30 m from the source is considered: the flux in the third harmonic is 95% of ideal and that of the fifth is 85%. A tuning curve showing the predicted on-axis brilliance for the first Undulator A is shown in Fig. 4. Those calculations take into account the emittance of the APS positron beam. As can be seen, a higher harmonic suffers a greater decrease in brilliance compared to the ideal case than a lower harmonic does, but the expected third harmonic brilliance is much closer to the ideal than the undulator specifications were designed to ensure.

The other relevant magnetic field characteristic - the variation of the field integrals through the undulator as the gap is changed - is also satisfactory. When the undulator was accepted, the high-order integrated multipoles were within the storage-ring requirements, as were the second integrals of the vertical and horizontal components of the field. Therefore, we were not concerned about their variation with gap. The first integral of the horizontal field was slightly larger than the storage-ring requirement, however, and the first integral of the vertical field varied by about 200 G-cm as the gap was changed through its full range. Glenn Decker, the storage-ring manager, desired a change of no more than 27 G-cm in the vertical first integral because at that value no correction or active feedback would be needed to keep the positron beam stable. Glenn will settle for 100 G-cm, though, and will use the active feedback system built into the storage ring to correct the positron beam orbit as needed. Note for comparison's sake that the earth's field integrated over the length of the undulator is about 120 G-cm.

Some magnetic fine tuning was carried out at the APS. After the fine tuning, the total variation in the first vertical field integral was reduced to 34 G-cm, as can be seen in Fig. 5.

In conclusion, the first Undulator A is expected to have a minimal effect on the stored positron beam, even when the undulator gap is changed. The x-ray spectrum from it will have a brilliance that is 93% and 80% of ideal for the third and fifth harmonics, respectively. It will also be able to span a greater range of photon energies than originally anticipated, because the minimum first harmonic energy will be 2.9 keV instead of 3.3 keV, and the fifth harmonic will be usable. We are very pleased with Undulator A #1 and eagerly await the arrival of the second!

Elizabeth R. Moog, Isaac Vasserman, Roger Dejus, and Didier Frachon ❖

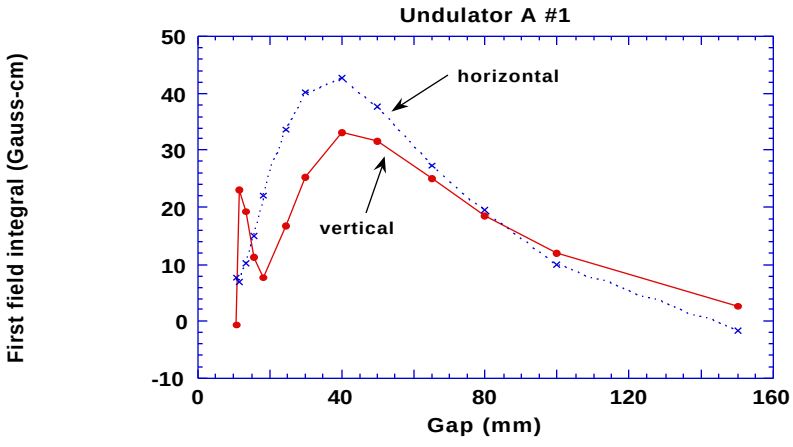

Fig. 5. The integrals along the undulator of the horizontal and vertical components of the magnetic field as a function of gap. The variation of the integrals with gap is small enough that no correction to the steering of the positron beam should be required as the gap is changed. For comparison, the integral of the vertical component of the earth's field along the undulator is 120 G-cm, and the integral of the field over a half period (i.e., over one peak) of the undulator is 9700 G-cm at minimum gap.

Dates to Remember

November 21, 1994
SRI CAT Meeting

December 23, 1994
thru January 2, 1995
Argonne Closed

Vacuum Protection of Beamline Front Ends at the Advanced Photon Source

The front end, which is immediately outside the storage ring but inside a concrete shielding wall of the APS, is designed to control and confine the photon beam and to provide both a vacuum barrier and interlock systems for personnel and equipment safety. For example, the APS ID front end for windowless operation has a differential pump (DP) to furnish a vacuum barrier. A safety shutter provides beam collimation during normal operation, as well as personnel protection from bremsstrahlung radiation. Two photon shutters are used to intercept the x-ray beam and protect the safety shutters and vacuum valves. Two fixed masks confine the x-ray beam and protect the downstream components from a missteered beam. A fast-closing valve provides quick vacuum protection in the case of a vacuum failure in the beamline. A slow valve provides a much better vacuum seal. Due to the high power of the APS photon beams, these front-end components are all conservatively engineered.

A mock-up of the ID beamline front end has been constructed, and various vacuum tests have been performed. Vacuum tests are needed because the front end has the same vacuum requirement as the storage ring (1×10^{-10} Torr without beam and 1×10^{-9} Torr with beam). The vacuum integrity is of utmost importance, especially in a windowless operation. In the following, we present results of vacuum tests conducted on the ID front-end mock-up.

First, small leaks of dry nitrogen were introduced into the downstream end of the differential pump through a leak valve. Three calibrated ionization gauges, located at the first photon shutter (PS1), the safety shutter (SS), and the downstream end of the DP, were used to measure the pressure distribution. The results were compared to those of finite element analyses.

Fig.1 shows the measured and calculated pressure distribution along the ID front-end mock-up. The system was pumped by ion pumps for three weeks but was not baked. The bottom curve shows the calculated result when no leak was introduced. The gas load at element 35 (7.5×10^{-9} Torr l/s) was solely due to thermal outgassing. To simulate small leaks, the thermal outgassing of element 35 is increased so that the calculated pressure matches the measured pressure. The middle curve shows the pressure profile when the gas load at element 35 was increased to 8.0×10^{-6} Torr l/s. The upper curve corresponds to a gas load of 7.6×10^{-5} Torr l/s. The measured pressures are represented by the symbols in the figure. Small leaks were introduced at element 35, and the pressure was stabilized for ~10 minutes before the ionization gauge readings were taken.

It is clear from Fig. 1 that the differential pump system is able to provide a vacuum barrier of almost three orders of magnitude. Aided by other pumps and the limited conductance of other components, the front end can handle a poor vacuum of 10^{-5} Torr in the beamline in a windowless configuration without affecting the storage-ring vacuum. The differential pump system will thus give the users full use of the ID beams at the APS.

The front-end vacuum protection system and trigger set points were designed as follows. Three conditions have to be satisfied to make the exit valve (denoted as EV, and located outside the shielding wall) open; namely, the pressure downstream of the DP or windows must be $< 1 \times 10^{-6}$ Torr, the pressure immediately upstream of the DP or windows must be $< 1 \times 10^{-8}$ Torr, and the pressure at the SS must be $< 6 \times 10^{-9}$ Torr. A cold-cathode vacuum gauge located between the shielding wall and the EV monitors the vacuum condition during operation. When the pressure reaches 1×10^{-8} Torr, trigger signals will be sent to close the PS1 and the slow valve (SV). As long as the pressure stays $< 1 \times 10^{-5}$ Torr, the beam will not be dumped. One can then close the EV and fix the problem without affecting other beamlines. If the pressure reaches 1×10^{-5} Torr however, the beam will be immediately dumped and the fast valve (FV) closed. In this case, the major concern is whether the SV and the FV can protect the storage-ring vacuum from large leaks so that the beam can be rapidly restored.

Experiments with large leaks have been carried out on the ID front-end mock-up. Regulated dry nitrogen was introduced into the downstream side of the mock-up through a mass flow controller (MFC) with a flow rate range from 0.1 to 10 slm (standard liter per minute). The gas-flow time was controlled by an air-actuated shut-off valve (V1). Four ionization gauges were installed in the mock-up. Gauge IG1 was located in a 8-inch 4-way cross, which was attached to the downstream side of the DP. Gauges IG2 to IG4 were located at the SS, PS2, and PS1, respectively. Ionization gauges respond to pressure changes in microseconds and thus give sufficient resolving capability. The analog signals from the ion gauges were recorded by a computer every millisecond when V1 was open. Shut-off valve V1 was triggered to open for only 10 s in each measurement.

Fig. 2 shows results of a typical measurement. The MFC was set at 1 slm with the regulator on the nitrogen cylinder at 30 psig. The gas flow overshot at first to over 10 slm when V1 was opened and then stabilized at 1 slm

within two seconds. The ion pumps were left on before the test. When V1 was triggered, all ionization gauges except IG4 were shut off by the incoming nitrogen wave. Related ion pumps at the DP, SS, and PS2 were also shut off when nitrogen arrived. The ion pump located between the FV and SV shut off after about two minutes, indicating that the FV was not vacuum tight, as expected. The SV however, protected the vacuum quite well. The pressure measured at IG4 increased slowly in ~3 s to 8.5×10^{-8} Torr but recovered to its original value within three minutes after the SV was closed. The kink in the IG4 curve at ~3800 m sec. (cf. Fig. 2) indicates the closing of the SV.

The gas shock-wave speed, counting from the first sign of pressure rise, is 191 m/s from IG1 to IG2. The shock- wave speed, measured from the point when the pressure reaches 1×10^{-5} Torr, is 65 m/s from IG1 to IG2. The rising time of IG2 (from 1×10^{-8} Torr to 8.5×10^{-5} Torr) is 25 ms.

Other measurements using different nitrogen flow rates indicate that the wave speed increases with increasing flow rate, as expected. A higher flow rate for the present test was obtained by removing the MFC and connecting the nitrogen cylinder directly to V1. With the regulator set at 50 psig, we have reached a nitrogen flow rate of ~156 slm, which is equivalent to an opening of a ~6-mm hole to the atmosphere in a 1-mm-thick window. In this case, the wave-front speed from IG1 to IG2 reached ~270 m/s, and the shock-wave speed increased to 98 m/s. The rise time of IG2 decreased to 22 ms. It still takes over 50 ms for the shock wave to reach the FV. The peak pressure at IG4 increased to 3.6×10^{-6} Torr. The vacuum at the first photon shutter recovered quickly to the 10^{-9} Torr range when the SV was sealed.

A shock-wave speed as high as ~1000 m/s has been reported in the literature for air propagation in a synchrotron beamline, which originated by the rupture of a large foil window (1×10 cm^2). By using baffles, a reduction by a factor of 3 - 5 in speed has been reported. In the APS front end, there are flow-limiting regions (apertures in the DP, vacuum chamber in the shielding wall, delay-line chamber and second fixed mask, etc.) interspersed with volume-expanding parts (ion pumps, SS, PS, etc.). This configuration forms an effective acoustic delay-line, which helps to reduce the shock-wave speed.

The fast valve is able to close within ~6.7 ms after triggering, which is sufficient to protect the storage-ring vacuum from even a catastrophic failure of a beryllium window in a beamline. The photon shutter (PS) closes within ~20 ms. This fast PS will be installed in the second-phase beamline front ends. A much slower, regular heavy-duty actuator with a closing time of ~3 s will be used in the first-phase beamline front ends. A fast PS will not help matters much if the closing time of the slow valve could not be shortened. The present technology allows only an improvement in closing time of slow valves to ~2 s. The good news is, even if we use the present slow valve, the front-end vacuum protection capability is sufficient.

The fast valve must be protected from the powerful x-rays by dumping the positron beam. Our experiments indicate that we can safely increase the trigger set point for the fast valve from 1×10^{-5} Torr to 1×10^{-3} Torr or higher to reduce the odds of beam dumping, since the APS front ends can handle much larger leaks.

In summary, a series of experiments have been carried out on a mock-up to test the front-end vacuum protection system. The controlled, small-leak experiments have shown good agreement between measured and calculated pressure distributions along the mock-up. The APS-designed differential pumping system for windowless configuration can provide a sufficient vacuum barrier with a large x-ray beam passage. The large-leak experiments demonstrate that the APS front-end vacuum protection system can handle leaks as large as 150 slm or more without significant damage to the storage-ring vacuum. The data also indicate that, even in a catastrophic window failure, the storage-ring vacuum is protected. These experiments provide valuable information for the optimization of the APS equipment protection system.

C. Liu, R. W. Nielsen, D. Shu, and T. M. Kuzay ❖

Look for the SRI CAT Logo Contest Results in the January Issue.

Welcome Newcomers!!!

Steve Brauer - Scientific Research Associate

Steve Brauer has joined the SRI CAT as a member of the X-ray Optics Group. Steve got his first taste of synchrotron radiation research while working for his Ph.D (McGill University). He gained further synchrotron radiation experience working as a postdoc at IBM under Brian Stephenson. Steve will be working with Brian Rodricks on our time-resolved program.

Zhonghou Cai - Scientific Research Associate

Sorry!!! Dr. Cai was incorrectly listed as a Postdoctoral Research Associate in the last issue.

Yiping Feng - Scientific Research Associate

Yiping Feng joined the scientific staff of Sector 2 in September of this year. Yiping, educated at Stanford and Pennsylvania State Universities, did his postdoctoral work with Exxon Research & Engineering Co. under Dr. S.K. Sinha. We welcome the strong experimental background in x-ray scattering and waveguides that he brings to SRI-CAT.

Mark Keeffe - Scientific Research Associate

Mark is responsible for the operation and maintenance of the 1-ID beamline. Prior to coming to the APS, Mark spent 8 years as an operator at CHESS, and has a wealth of practical synchrotron experience. Mark is a 1984 graduate of Notre Dame.

Sarvjit Shastri - Postdoctoral Research Associate

Sarvjit is a postdoc working on the high-energy x-ray program with Dean Haeffner. He comes to the APS from Cornell University where his thesis (under Prof. Batterman) was on "X-ray Polarization Optics and Coherent Nuclear Resonance Scattering Using Synchrotron Radiation." He has a BS in Applied Physics from the California Institute of Technology (1988).

Klaus Quast - Scientific Research Associate

Klaus Quast is a scientific research associate working with staff members on Sector 3 of the SRI CAT. Klaus was trained in electromechanics and was awarded a Master of Science degree in Physics from the University of Hamburg in Germany. He comes to the APS with experience gained from his position as Scientific Associate at the University of Hamburg.

Publications

Barraza, J., D. Shu, and T. M. Kuzay, Front End Support Systems for the Advanced Photon Source, Nucl. Instrum. Meth. Phys. Res. A347 (1994) 591-597.

Blasdell, R. C., A. T. Macrander, and W.-K. Lee, A Ray-Tracing Study of Inclined Double-Crystal Monochromators, Nucl. Instrum. Meth. Phys. Res. A347 (1994) 327-330.

Blasdell, R. C., and A. T. Macrander, Modifications to the 1989 SHADOW Ray-Tracing Code for General Asymmetric Perfect-Crystal Optics, Nucl. Instrum. Meth. Phys. Res. A347 (1994) 320-323.

Dejus, R. J., Computer Simulations of the Wiggler Spectrum, Nucl. Instrum. Meth. Phys. Res. A347 (1994) 56.

Dejus, R. J., and A. Luccio, Program UR: General Purpose Code for Synchrotron Radiation Calculations, Nucl. Instrum. Meth. Phys. Res. A347 (1994) 61.

Dejus, R.J., Lai, B., Moog, L., and Gluskin, E., Undulator A Characteristics and Specifications: Enhanced Capabilities, *Technical Bulletin* **ANL/APS/TB-17** (Argonne National Laboratory, 1994).

Huang, Q., R. Hopf, and B. Rodricks, A VXI-Based High Speed X-ray CCD Detector, Nucl. Instr. and Meth. in Phys. Res. A348 (1994) 645-648.

Kushnir, V. I., and A. T. Macrander, A Criterion for the Dynamical-to-Kinematical Transition in X-ray Diffraction by a Bent Crystal, Nucl. Instrum. Meth. Phys. Res. A347 (1994) 331-337.

Kuzay, T. M., A Review of Thermo-Mechanical Considerations of High Temperature Materials for Synchrotron Applications, Nucl. Instrum. Meth. Phys. Res. A347 (1994) 644-650.

Lang, J. C., X. Wang, V. P. Antropov, B. N. Harmon, A. I. Goldman, H. Wan, G. C. Hadjipanayis, and K. D. Finkelstein, Circular Magnetic X-ray Dichroism in Crystalline and Amorphous $GdFe_2$, Phys. Rev. B 49 (1994) 5993-5998.

Lee, W.-K., and D. M. Mills, High Heat Load X-ray Optics Research and Development at the Advanced Photon Source — an Overview, Nucl. Instrum. Meth. Phys. Res. A347 (1994) 618-626.

Macrander, A. T., and R. C. Blasdell, Weak Polarization Effects for an Inclined Crystal Monochromator, Nucl. Instrum. Meth. A347 (1994) 324-326.

McNulty, I., The Future of X-ray Holography, Nucl. Instrum. Meth. A347, (1994) 170.

McNulty, I., X-ray Intensity Interferometry with a Short-Pulse FEL, *Technical Report* **SLAC-437**, 249 (SSRL, Stanford University 1994)

Nian, H. L. T., D. Shu, I. C. A. Sheng, and T. M. Kuzay, Thermo-Mechanical Analysis of Fixed Mask 1 for the Advanced Photon Source Insertion Device Front Ends, Nucl. Instrum. Meth. Phys. Res. A347 (1994) 657-663.

Rodricks, B., Q. Huang, R. Hopf, and K. Wang, A Large Area Detector for X-ray Applications, Nucl. Instr. and Meth. in Phys. Res. A348 (1994) 572-576.

Rogers, C.S., Mills, D.M., and Assoufid, L., The Cryogenic Cooling Program at the Advanced Photon Source, *Technical Bulletin* **ANL/APS/TB-18**, (Argonne National Laboratory, 1994).

Smither, R. K., and P. B. Fernandez, Symmetric-Cut Monochromator with Adjustable Asymmetry, Nucl. Instrum. Meth. Phys. Res. A347 (1994) 313-319.

Smither, R. K., and P. B. Fernandez, Apparent Temperature Versus True Temperature of Silicon Crystals as a Function of Their Thickness Using Infrared Measurements, Nucl. Instrum. Meth. Phys. Res. A347 (1994) 640-643.

Sturhahn, W., and E. Gerdau, Evaluation of Time-Differential Measurements of Nuclear- Resonance Scattering of X-rays, Phys. Rev. B 49 (1994) 9285-9294.

Wang, Z., T. Nian, D. Ryding, and T. M. Kuzay, Low-Cycle-Fatigue Behavior of Copper Materials and Their Use in Synchrotron Beamline Components, Nucl. Instrum. Meth. Phys. Res. A347 (1994) 651-656.

Yahnke, C., G. Srajer, D. R. Haeffner, D. M. Mills, and L. Assoufid, Germanium X-ray Phase Plates for the Production of Circularly Polarized X-rays, Nucl. Instrum. Meth. A347 (1994) 128-133.

Yoo, S. S., K. Wang, P. A. Montano, J. P. Faurie, Q. Huang, and B. Rodricks, Fast Photoconductor CdTe Detectors for Synchrotron X-ray Studies, Nucl. Instrum. and Meth. Phys. Res. A348 (1994) 527-530.